The Production of Butyl Acetate and Methanol via Reactive and Extractive Distillation. I. Chemical Equilibrium, Kinetics, and Mass-Transfer Issues

ARTICLE *in* INDUSTRIAL & ENGINEERING CHEMISTRY RESEARCH · NOVEMBER 2002

Impact Factor: 2.59 · DOI: 10.1021/ie0107643

3 AUTHORS, INCLUDING:

Laureano Jiménez
Universitat Rovira i Virgili
180 PUBLICATIONS **1,197** CITATIONS

The Production of Butyl Acetate and Methanol via Reactive and Extractive Distillation. I. Chemical Equilibrium, Kinetics, and Mass-Transfer Issues

Laureano Jiménez,*,† Alfonso Garvín, and José Costa-López

Department of Chemical Engineering and Metallurgy, University of Barcelona, c/Martí i Franqués 1, 08028 Barcelona, Spain

We studied the kinetic and chemical equilibrium of the transesterification of methyl acetate with *n*-butanol in a batch stirred-tank reactor with a polymeric acid resin as a catalyst. The aim of this work was to determine whether reactive and extractive distillation is a promising alternative for managing a byproduct from the poly(vinyl alcohol) process. The experiments were performed in concentration and temperature ranges similar to those predicted for operation. The entrainer (*o*-xylene) was observed to have no influence on the kinetics. Internal and external mass-transfer resistances were found to be negligible under the operating conditions considered. The experimental results were best described (average error of 2%) by a pseudohomogeneous model with a first-order dependency on the reactants. The influence of the temperature was modeled with the Arrhenius equation. The forward and reverse kinetic constants were consistent with the chemical equilibrium values.

Introduction

The use of unit operations separately and consecutively to achieve cost-effective conversion requires high reflux ratios and prohibitive recycle flow rates. Reactive separation processes such as reactive distillation, reactive absorption, and reactive crystallization have attracted growing interest as promising alternatives in both industrial applications and scientific research. This paper focuses on reactive distillation, a technology that is particularly suited for reversible reactive systems in which chemical equilibrium limits the conversion. Other advantages are that side reactions can be bypassed, the limitations of azeotropic mixtures can be overcome, hot-spot problems can be avoided, and the heat of reaction can be used for selective product removal.[1] These synergistic effects mean that reactive distillation can have significant economic advantages over a conventional design. Although reactive distillation is not advantageous in every case (e.g., reaction rates must be similar to those in a reactor at pressures suitable for distillation), it is commonly used for etherification and esterification reactions, although it has been fruitfully applied to alkylation, nitration, and amidation processes. Reactive distillation has been proposed for methyl acetate (MeAc) hydrolysis,[2,3] and it is used as a model for research. A very useful designer's checklist has been published by Hoshang and Fair.[4] In addition, a complete list of references, classified as patents, thermodynamic properties, and case studies can be found in the work by Hauan.[5]

* To whom correspondence should be addressed. Tel.: +34-977-559617. Fax: +34-977-559667/21. E-mail: ljimenez@etseq.urv.es.

† Present address: Department of Chemical Engineering, ETSEQ, University Rovira i Virgili, Av. dels Països Catalans 26, 43007 Tarragona, Spain.

Problem Statement

We developed a new process to recover MM20, a byproduct from the poly(vinyl alcohol) industry. On one hand, a byproduct processing plant is more elaborate and costly today than ever before, because quality requirements are severe. On the other hand, a recovery system is a business opportunity.

MM20, a mixture of MeOH and MeAc rich in MeOH (∼30 wt % MeAc), is first converted into MM80 (∼80 wt % MeAc, 0.05 wt % maximum water content, and 0.05% maximum acidity). The objective is to process the MM80 by reactive distillation with *n*-butanol (BuOH) and obtain high-purity MeOH and butyl acetate (BuAc). Despite volatile organic carbon legislation, BuAc consumption is expected to grow in the near future.[6] The overall process can be represented by

$$\mathrm{MeAc} + \mathrm{BuOH} \leftrightarrow \mathrm{BuAc} + \mathrm{MeOH}$$

The problem is that the system simultaneously has a low chemical equilibrium extent and several azeotropes. To eliminate azeotropes, two techniques are widely used: pressure swing distillation, which changes the system composition and moves the distillation boundaries, or entrainers, which modify the relative volatility. In our case, the solvent goal aims to break the azeotropes and improve contact between the reactants in the reactive section of the reactive and extractive distillation (RED) unit.

No kinetic or chemical equilibrium data were available in the literature, and although they can be estimated from group contribution methods,[7,8] experimental data are strongly recommended, particularly when product specifications are based on maximum impurities.

The literature[9,10] shows that heterogeneous catalysts such as sulfonated macroporous ion-exchange resins accelerate esterification. Resins provide products of constant quality and minimize wastewater and corro-

10.1021/ie0107643 CCC: $22.00
Published on Web 11/16/2002

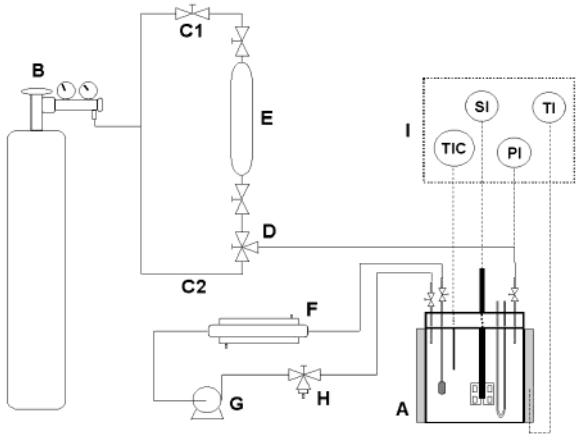

Figure 1. Schematic diagram. A, batch stirred-tank reactor; B, nitrogen cylinder; C1 and C2, flow paths; D, three-way valve; E, container; F, heat exchanger; G, pump; H, sample point; I, control monitor.

sion problems. The main drawbacks are the low thermal stability, the need for catalyst containers to improve mechanical properties, and the possibility of diffusion problems. Resins are also susceptible to both short-term poisoning and long-term deactivation.

The first part of this paper focuses on chemical equilibrium and kinetic aspects, using a similar approach to that of Pöpken et al.[11] The design of reactive distillation is currently based on expensive and time-consuming sequences of laboratory and pilot-plant experiments. The second part[12] presents the RED unit and the solvent recovery system design and dynamic modeling. Recently, Castor et al.[13] and Podrebarac et al.[14] have used similar approaches for various applications.

Experimental Work

Chemicals. E. Merck (Darmstadt, Germany) supplied the chemicals. MeOH and BuOH were Uvasol spectroscopy-grade (purity > 99.9 wt %), and MeAc and BuAc were high-purity (purity > 99.8 wt %). *o*-Xylene (purity > 99.0 wt %) and *N*,*N*-dimethylformamide (purity > 99.0 wt %) were distilled twice in a packed column, and their final purities were 99.6 and 99.8 wt %, respectively. The substances were dried with Union Carbide 3 Å molecular sieves, provided by Fluka AG (Buchs, Switzerland). All purities were checked by gas chromatography.

Catalyst. Amberlyst 15,[13] a sulfonic ion-exchange resin (exchange capacity of 4.81 $mol_{H^+} \cdot kg^{-1}$), manufactured by Rohm & Haas (Philadelphia, PA), was used as catalyst. Before the experiments, the catalyst was dried at 95 °C for 24 h to remove the water from the pores. Under these conditions,[15] the equilibrium moisture is less than 1 wt %, and therefore, no hydrolysis reaction occurs.

Apparatus. Figure 1 shows a schematic diagram of the setup. The experiments were conducted in a stainless steel stirred-tank reactor (FC-3 model, 300 mL) manufactured by Pressure Products Industries (Warminster, PA). The unit was equipped with a turbine motor and a digital tachometer speed controller (Dyna/Mag model MM-016-06). The temperature was measured with PT-100 thermometers (accuracy of ±0.1 K) and controlled by a PID within ±0.2 K with a potentiometer. The pressure indicator was a digital manometer (±0.1 kPa). A filter (45-μm) was used to prevent any of the catalyst from being dragged into the external recycle. The external pump was a Tuthill series D model (Alsip, IL).

Analysis. The analyses were carried out in a Hewlett-Packard (Palo Alto, CA) 5890 Series II Plus gas chromatograph, equipped with an FID and electronic pressure control. The capillary column was a Supelco 2-4159 column with a 1-μm PTE-5 film (30 m, 0.0032-mm i.d.) with helium as the carrier gas.

Procedure. The experiments were conducted in a thermostated batch reactor that was overpressurized (10 atm) to maintain all of the chemicals in the liquid phase.

To fix the starting point of the kinetic experiments precisely, the following procedure was used. First, the reactor (A) was filled with the solvent, the nonreactive mixture, and the catalyst. Then, the system was heated to the temperature set point, and the pressure was fixed at around 3−4 atm under the working conditions with nitrogen (B) by C1. When the required temperature was reached, the three-way valve (D) was switched, and the pressure increased; the nitrogen passed through C2 and pushed the reactant (E) into the reactor. The external recycle stream was cooled with a heat exchanger (F) before it entered the pump (G) to prevent any flashing at the sample point (H). The residence time in the external recycle loop (line F−G−H) was less than 1.5 min, and this influence was neglected compared with the long kinetic and chemical equilibrium experiments. The initial composition was known from the first analysis. Samples were taken every 5 min at the beginning of the experiments and every 20−30 min thereafter (8−12 samples per test) to monitor the progress of the reaction. The amount of sample was around 1−2 mL. TIC, PI, TI, and SI (I) controlled and monitored the system's operating variables.

Experimental Plan. Various experiments were carried out starting from different compositions: (a) alcohol, ester, and entrainer mixtures, because forward and backward reactions occur simultaneously; (b) mixtures with MM80 as the feed; and (c) mixtures with different *o*-xylene concentrations, because of the possible influence of *o*-xylene on catalyst activity.

The thermal stability of the catalyst restricts the operating temperature to 90−95 °C. Preliminary simulation results predicted that temperatures in the RED unit should be higher than 50 °C to achieve measurable reaction rates.

The kinetic experiments lasted for 5−6 h (∼1.5 wt % catalyst), whereas the equilibrium experiments lasted for 9−12 h (∼6.5 wt % catalyst). Over 40 equilibrium and 25 kinetic experimental runs were made to evaluate the effects of catalyst concentration, stirrer speed, catalyst size, temperature, and chemical concentration.

Results

During the experiments, no loss of catalytic activity or damage by swelling forces was observed. A set of five experiments was performed with the same catalyst, and no difference in activity was observed. Nevertheless, the catalyst was discarded after each experiment. The molar yields calculated from the analytical results for replicate experiments always agreed to within a few percent (±3%). Equilibrium and kinetic expressions were derived separately, and their coincidence was used as a global consistency test.

Table 1. Binary Parameters for the NRTL Activity Coefficient Model

system	b_{12} (K)	b_{21} (K)	α_{12}
MeAc + BuOH	−3897.4	1567.7	0.30
MeOH + *o*-xylene	447.17	516.01	0.30
BuOH + *o*-xylene	130.32	387.12	0.30
BuAc + *o*-xylene	−18.438	63.604	0.30

Table 2. Solvation and Association Parameters for the Hayden and O'Connell Method

	MeOH	MeAc	BuOH	BuAc	*o*-xylene
MeOH	1.63				
MeAc	1.30	0.85			
BuOH	1.55	1.30	2.20		
BuAc	1.30	0.53	1.30	0.53	
o-xylene	0.00	0.60	0.00	0.60	0.00

Estimation of Physical Properties. The activity coefficients were estimated by NRTL,[16] with temperature-dependent interaction parameters (eqs 1 and 2). Vapor-phase nonidealities were calculated using Hayden and O'Connell's method.[17] Any other parameter used was retrieved from the Aspen PLUS Database.[18] No VLE data was found in the literature for the key systems (except MeAc + BuOH), and $T-x-y$ measurements were performed.[19,20] The parameters are shown in Tables 1 and 2.

$$G_{ij} = \exp(-\alpha_{ij}\tau_{ij}) \tag{1}$$

$$\tau_{ij} = a_{ij} + \frac{b_{ij}}{T} \tag{2}$$

where G_{ij}, α_{ij}, τ_{ij}, a_{ij}, and b_{ij} are the interaction parameters in the NRTL model. We found experimental evidence of pseudoazeotrope behavior for the methanol + *o*-xylene system at high methanol composition (not predicted by UNIFAC). This aspect is addressed in more detail in part II of this paper.[12]

Residue Curve Map Analysis. Residue curve maps (RCMs) have been successfully applied to complex nonideal separation systems and provide valuable insights and design assistance for a variety of separation processes. RCMs are based solely on the system's physical properties: vapor−liquid equilibrium, liquid−liquid equilibrium, and solubility data. The number and type of singular points is unknown a priori. The temperature always increases along a residue curve line, and the singular points are either nodes (stable or unstable) or saddles. The role of the singular points can be assigned using Doherty and Perkins' rules,[21] and the topology for the whole composition space can be stated. This makes RCM a promising technique in the early phase of development of any project. Aspen SPLIT[22] was used to compute the RCM.

An accurate analysis of the quaternary nonreactive RCM diagram (Figure 2) reveals that there are two distillation regions. The MeOH + MeAc azeotrope acts as an unstable node, and BuAc and BuOH are both stable nodes, whereas MeOH and the BuOH + BuAc azeotrope are both saddles. Any of the four feasible distillation sequences detected lead to the desired separation. These two aspects show that it is advisable to use either a boundary-crossing strategy or an entrainer to separate the products.

Extractive Distillation. Solvent selection is the key factor in RED, as the entrainer objective is to break the azeotropes and the solvent recovery system has considerable influence on the process performance.[23] The huge number of possible solvents has led to some previous selections being made on the basis of heuristics.[2,24]

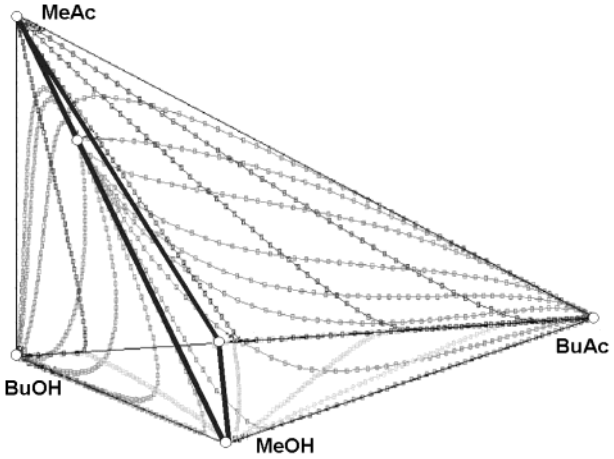

Figure 2. Nonreactive RCM for the MeAc + BuOH + BuAc + MeOH system at 101.3 kPa.

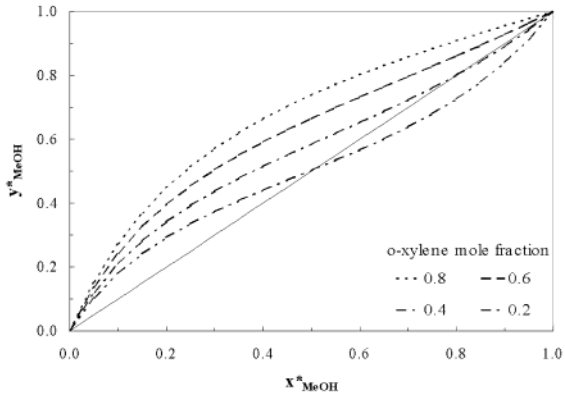

Figure 3. Influence of *o*-xylene on the vapor−liquid equilibrium of the MeOH + MeAc system 101.3 kPa. $x_i^* = x_i/\sum_j x_j$, i, j = MeOH, MeAc ($\sum_j x_i^* = 1$).

The most commonly accepted parameter for solvent selection is selectivity.[25] The higher the selectivity, the better the solvent. Different entrainers are compared by considering the situation at infinite dilution, as stated in eq 3

$$S_{ij,S}^{\infty} = \frac{\gamma_{i,S}^{\infty}}{\gamma_{j,S}^{\infty}} \tag{3}$$

Experimental work using headspace gas chromatography was done for alcohol + acetate + entrainer systems.[26] The $S_{m,S}^{\infty}$ criterion is useful for clustering the solvents into different groups, but a definitive selection criterion cannot be stated. The experimental results show that the best entrainers are alkylbenzenes and alkanes. Also, the importance of peripheral properties (e.g., safety, cost, density), that is, properties that are of interest when selecting a solvent but that often do not directly affect the separation, was discussed. When all of these considerations and parameters had been weighed, *o*-xylene was selected as the best alternative. Figure 3 shows the MeOH + MeAc + *o*-xylene pseudobinary diagram. This diagram was used to compute the minimum entrainer concentration required to break the binary azeotrope. Moreover, an analysis of the space composition of the five-component system residue curve

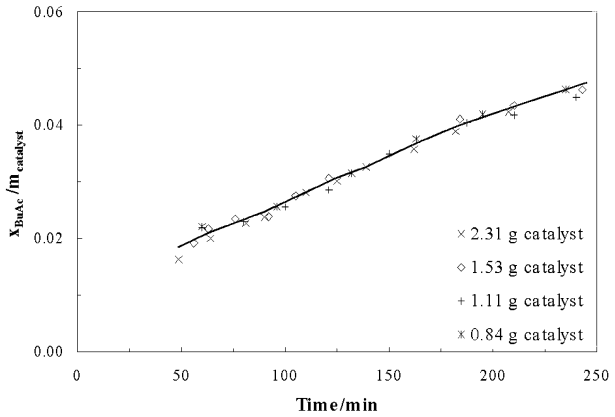

Figure 4. Influence of the amount of catalyst on the BuAc rate of formation.

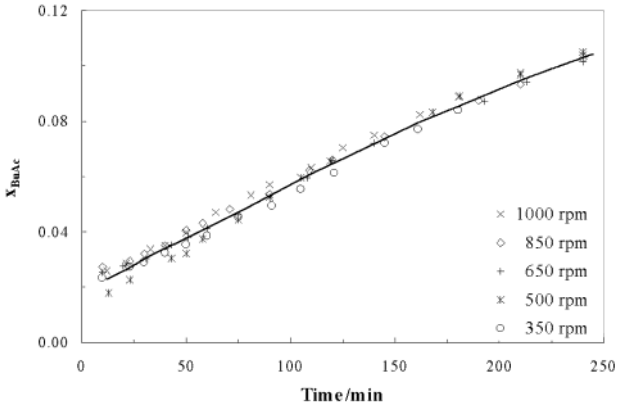

Figure 5. Effect of the stirring speed on the BuAc rate of formation.

map reveals that there is just one distillation region, where *o*-xylene and the MeOH + MeAc azeotrope are the stable and unstable nodes, respectively.

Entrainer Influence. Amberlyst 15 was selected as the catalyst because of its capacity to work in anhydrous and nonpolar conditions. The sulfonic groups give the resin a strong affinity for polar molecules, which are preferentially adsorbed, and inhibit the adsorption of *o*-xylene. Moreover, as MM80 is water-free, the possible reduction of the available catalyst active sites is minimized. Neither the chemical equilibrium nor the kinetic results shows dispersion depending on the initial composition.

External and Internal Mass Transfer Effects. The reactants and products must be transported throughout the catalyst pores and inside the gel beads where 95% of the acid sites are located.[27] Diffusion phenomena, therefore, can have an enormous effect on the results. The reactions are slightly endothermic, and the catalyst particles can be considered to be essentially isothermal. The heat of mixing was also not found to have any influence.

Three full sets of experiments were carried out with different amounts of catalyst (Figure 4), different agitation velocities (Figure 5) and different sieved fractions of the catalyst (Figure 6). All experiments were performed at 80 °C and 10 bar. Figure 5 shows a minor influence of the stirring speed, but the discrepancy is in the range of the error of this technique. Figure 6 shows that, for high *o*-xylene concentrations (thus, low conversion), no diffusion problems were found. The main conclusion is that the external and/or internal mass-

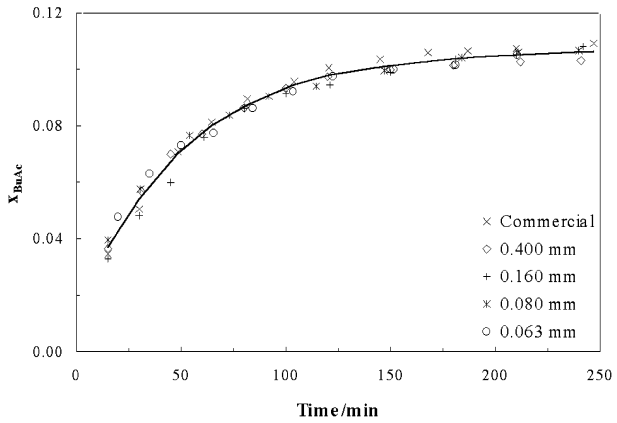

Figure 6. Impact of the catalyst particle size diameter on the BuAc rate of formation.

transfer diffusion exerts no influence. As a secondary conclusion, we can state that the reproducibility is very high. A qualitatively theoretical verification of mass-transfer resistance was made using the dimensionless Biot number and the Thiele modulus.[28] The results provided by the Biot number confirm that the transport across the liquid−solid interface is over 1 order of magnitude larger than the transport inside the pores of the catalyst. Also, the low Thiele modulus values (between 0.058 at 60 °C and 0.363 at 90 °C) had a corresponding effectiveness factor that is virtually 1 (>0.95). In accordance with the results from this section, in the subsequent experimental work, we used unsieved catalyst particles and a stirring speed of 1000 rpm.

Side Reactions. The values of the equilibrium constants were estimated using Aspen PLUS (Aspen Technology Inc., Cambridge, MA), by minimizing the Gibbs free energy. As all chemicals were water-free, the conversions caused by hydrolysis were expected to be insignificant. Gas chromatographic analysis confirmed that the formation of such byproducts as dimethyl ether by dehydration of MeOH or acetic acid by hydrolysis was negligible (less than 0.01 wt %).

Chemical Equilibrium Experiments. For a homogeneous system with an equilibrium reaction in the liquid phase, the equilibrium constant can be written as[28]

$$K_a = \prod \gamma_i^{\nu_i} \prod x_i^{\nu_i} \prod \left[\frac{f_i}{f_i^o}\right]^{\nu_i} = K_\gamma K_x K_f \qquad (4)$$

Therefore, the equilibrium constant can be expressed as the product of the activity coefficient constant (K_γ), the liquid molar fraction constant (K_x), and the fugacity constant (K_f). Although the entrainer has a significant effect on the activity coefficients and equilibrium temperatures, its influence on the activity coefficient constant is negligible (Table 3). As expected, the K_f variation was insignificant, but it was still taken into consideration in the calculations.

The chemical equilibrium constant under standard conditions can be derived from the Gibbs free energy, yielding the equation

$$\ln K_a = \frac{\Delta S^o}{R} - \frac{\Delta H^o}{R}\frac{1}{T} \qquad (5)$$

Equation 5 is valid assuming that the heat of reaction is constant over the temperature range (experiments

Table 3. Activity Coefficient Equilibrium Constant at Different Temperatures at 10 atm

	MeAc	BuOH	BuAc	MeOH	*o*-xylene
x_{eq} (mol)	0.1320	0.1976	0.0461	0.3698	0.2545
γ_{eq}	1.3156	1.1641	1.2959	1.4387	1.9687
k_γ			1.2174		
T_{eq} (K)			338.15		
x_{eq} (mol)	0.1682	0.1428	0.0637	0.2049	0.4204
γ_{eq}	1.1702	1.5234	1.0424	2.1177	1.3892
k_γ			1.2382		
T_{eq} (K)			323.15		
x_{eq} (mol)	0.0896	0.0884	0.0532	0.1096	0.6592
γ_{eq}	1.2555	2.0367	1.0354	3.1378	1.1224
k_γ			1.2705		
T_{eq} (K)			353.15		
x_{eq} (mol)	0.2792	0.1716	0.1368	0.2954	0.1169
γ_{eq}	1.1891	1.2191	1.2101	1.4614	1.9686
k_γ			1.2198		
T_{eq} (K)			363.15		

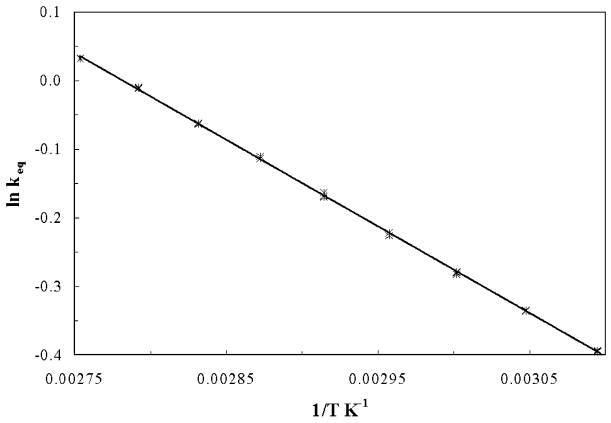

Figure 7. Dependence of the chemical equilibrium constant on temperature for the transesterification of MeAc with BuOH.

were performed every 5 °C between 50 and 90 °C). Analyses with liquid temperature-dependent heat capacities were performed (the parameters were retrieved from the Aspen PLUS database). Using temperature-dependent heat capacities or constant heat capacities, the model predictions fit the data very well ($r^2 = 0.9968$ and $r^2 = 0.9993$, respectively), because the heat capacities of the reactants and products are almost constant. ΔH^o values (10 510 ± 141 and 11 570 ± 149 J·mol^{-1}, respectively) and ΔS^o values (29.25 ± 0.49 and 31.22 ± 0.51 J·mol^{-1}, respectively) were coincident, and the simpler expression was preferred. Figure 7 shows the K_a dependence on temperature. For example, the theoretical standard heat of reaction is 4800 J·mol^{-1},[18] about the same order of magnitude as the experimental value, although the experimental error associated with this technique can have values around 1 kJ·mol^{-1}.

Equilibrium conversion starting from different feed ratios was completed. An iterative method that computed calculations with Aspen PLUS in the inner loop (activity and fugacity coefficients) was used, while concentration calculations were performed in the outer loop. The equilibrium conversion for the MeOH + MeAc azeotrope and stoichiometric BuOH ranged between 31 and 36% over the temperature range studied. These results confirms that RED can be used to circumvent the chemical equilibrium constraint.

Kinetic Experiments. We evaluated the effects of the temperature, the reagent concentration, and the entrainer on the reaction rate (Table 4). Figure 4 shows that the reaction rate is proportional to the amount of catalyst and that the reaction rate can be affected by

Table 4. Experimental Runs for the Kinetic Experiments[a]

set	catalyst (g)	T (°C)	initial mixture
1[b]	0.451	90	reagent-rich
2	1.428	90	product-rich
3[b]	2.048	90	MM80
4	1.349	80	reagent-rich
5	2.003	80	product-rich
6[b]	2.028	80	MM80
7[b]	2.323	80	MM80
8[b]	0.451	70	reagent-rich
9	2.136	70	product-rich
10[b]	3.542	70	MM80
11[b]	0.541	60	reagent-rich
12	1.555	60	product-rich
13[b]	2.026	60	MM80

[a] Conditions: 10 bar, 1000 rpm, and commercial catalyst. [b] Triplicate experiment.

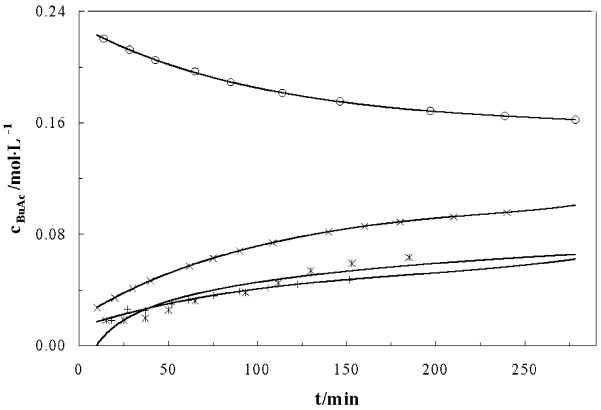

Figure 8. BuAc concentration profile at 80 °C for the transesterification of MeAc with BuOH.

using this amount as the basis. The SPSS software package capabilities[29] were used to carry out the regressions.

The tools and regression techniques used (generalized reduced gradient) were not able to simultaneously fit all of the parameters of the Langmuir−Hinselwood−Hougen−Watson (LHHW) equation, no matter which adsorption mechanism was selected.[28] Different sets of absorption k values with different orders of magnitude exhibit approximately the same error. This situation can be partially justified for coupling effects in the different adsorption terms.

The pseudohomogeneous model with a second-order expression (eq 6) was in good agreement with the experimental data. The power-law model did not significantly improve the predictive capabilities, as the upgrade does not justify the need for four additional parameters. Some authors[3,4,6,14,27] have already drawn similar conclusions for the hydrolysis, esterification, and transesterification of alcohols and acetates. We assumed an Arrhenius-type temperature dependence for both the direct and reverse constants.

$$r = kc_{MeAc}c_{BuOH} - k'c_{BuAc}c_{MeOH} \qquad (6)$$

Experimental profiles were obtained (Table 4) for each experiment. For the sake of illustration, Figure 8 shows the runs at 80 °C with experiments in which both forward and reverse reactions prevail. At 50 °C, because of the small absolute value of the reaction rate, slight deviations lead to high relative errors, and therefore, these data sets were not used. Figure 9 shows the direct

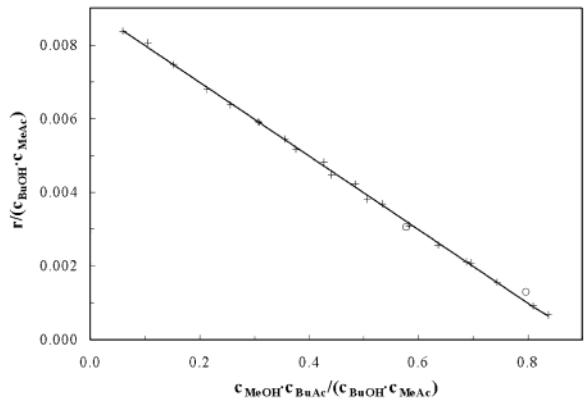

Figure 9. Fit of forward and reverse kinetic constants at 90 °C for the transesterification of MeAc with BuOH.

Table 5. Temperature Dependence of the Forward and Reverse Kinetic Constants

T (°C)	k ($L \cdot mol^{-1} \cdot min^{-1} \cdot g_{cat}^{-1}$)	k' ($L \cdot mol^{-1} \cdot min^{-1} \cdot g_{cat}^{-1}$)
60	$1.044 \times 10^{-3} \pm 4.55 \times 10^{-6}$	$1.145 \times 10^{-3} \pm 2.49 \times 10^{-5}$
70	$2.283 \times 10^{-3} \pm 1.59 \times 10^{-4}$	$2.457 \times 10^{-3} \pm 2.74 \times 10^{-5}$
80	$4.563 \times 10^{-3} \pm 6.98 \times 10^{-5}$	$5.040 \times 10^{-3} \pm 3.13 \times 10^{-5}$
90	$8.989 \times 10^{-4} \pm 6.58 \times 10^{-5}$	$1.001 \times 10^{-2} \pm 1.30 \times 10^{-4}$

Table 6. Arrhenius Constants for the Forward and Reverse Reactions

	A ($L \cdot mol^{-1} \cdot min^{-1} \cdot g_{cat}^{-1}$)	E_a ($kJ \cdot mol^{-1}$)
k	$2.018 \times 10^{8} \pm 2.1 \times 10^{7}$	71.96 ± 2.7
k'	$2.839 \times 10^{8} \pm 4.6 \times 10^{7}$	72.67 ± 0.46

Table 7. Error in the Estimation of the Transesterification Reaction Rate

T (°C)	$\overline{\Delta r}$ (%)	Δr_{max} (%)
60	1.13	2.45
70	2.31	3.92
80	2.43	5.63
90	1.37	3.51

and reverse kinetic fitting for the set of experiments conducted at 90 °C.

The regressed kinetic parameters for the pseudohomogeneous model (eq 6) and the dependence of this parameter on temperature are shown in Table 5. These values follow the Arrhenius model, and the results are provided in Table 6. It is noteworthy that, although the forward and reverse reactions had similar coefficients of determination (over 0.99 in both cases), the Fisher distribution values (F) were significantly different (13 517 and 45 331, respectively). The F value is an indicator that considers the variance taken into account by the model and the number of parameters: high F values indicate better models.[29] This factor and the inherent problem of regressing logarithmic values lead to high relative errors in some parameter estimates (see Table 7). The values for the equilibrium constant and the kinetic parameters are similar to those found for the transesterification of MeAc with ethanol.[30]

Conclusions

Reaction kinetics, chemical equilibrium, and mass-transfer issues have been evaluated for the transesterification of MeAc with BuOH, where the yield is strongly limited by the equilibrium conversion. The advantage of using an acid resin catalyst is that very few byproducts are formed. *o*-Xylene was identified as a suitable extractive agent, and it was used as the reaction solvent. The operating conditions were such that the control step was the reaction at the catalyst surface, and therefore, the kinetic expression was considered to be essentially representative of the intrinsic rate of reaction and free of mass-transfer effects. The pseudohomogeneous kinetic model proved to have very good predictive capabilities (average errors around 2%). Equilibrium and kinetic results were consistent ($K_a \approx k/k'$). The effects of temperature and composition were studied so that an expression could be developed to model the RED unit in part II of this paper.[12]

Acknowledgment

The authors thank DGICYT and CIRIT for providing the necessary facilities and A. Destro (UTN, Panama) and R. Peis (UTM, Germany) for carrying out some of the experiments. Some of the authors (L.J. and A.G.) gratefully acknowledge the financial support from Fundación Caja de Madrid.

Notation

a_{ij} = interaction parameter in the NRTL model
A_i = preexponential factor, $L \cdot mol \cdot min \cdot g_{cat}^{-1}$
b_{ij} = interaction parameter in the NRTL model, K^{-1}
c_i = molar concentration, $mol \cdot L^{-1}$
E_a = activation energy, $kJ \cdot mol^{-1}$
F = Fisher distribution value (significance = 95%)
f_i = fugacity, Pa
G_{ij} = interaction parameter in the NRTL model
ΔG = Gibbs free energy of formation, $J \cdot mol^{-1}$
ΔH = enthalpy, $J \cdot mol^{-1}$
K_a = chemical equilibrium constant
MM20 = byproduct from the poly(vinyl alcohol) process
MM80 = azeotropic mixture of MeOH + MeAc from the poly(vinyl alcohol) process
r = reaction rate, $mol \cdot L^{-1} \cdot min^{-1} \cdot g_{cat}^{-1}$
RCM = residue curve map
RED = reactive and extractive distillation
rpm = revolutions per minute
S_i = selectivity
ΔS = entropy, $J \cdot mol^{-1} \cdot K^{-1}$
T = temperature, K or °C
x_i, y_i = liquid/vapor phase molar fractions
x_i^*, y_i^* = liquid/vapor phase pseudobinary molar fractions

Greek Symbols

α_{ij} = interaction parameter in the NRTL model
γ_i = liquid-phase activity coefficient
τ_{ij} = temperature-dependent interaction parameter in the NRTL model
ν_i = stoichiometric coefficient

Subscripts and Superscripts

i, j = ith and jth components, respectively
m = multicomponent
o = standard state/conditions
S = in the presence of solvent
∞ = infinite dilution
$-$ = mean value
$'$ = reverse reaction
* = pseudobinary basis

Literature Cited

(1) Malone, M. F.; Doherty, M. F. Reactive Distillation. *Ind. Eng. Chem. Res.* **2000**, *39*, 3953.

(2) Agreda, V. H.; Partin, L. R.; Heise, W. H. High Purity Methyl Acetate via Reactive Distillation. *Chem. Eng. Prog.* **1990**, *86*, 40.

(3) Fuchigami, Y. Hydrolysis of Methyl Acetate in Distillation Column Packed with Reactive Packing of Ion Exchange Resin. *J. Chem. Eng. Jpn.* **1990**, *23*, 354.

(4) Hoshang, S.; Fair, J. R. Design Guidelines for Solid-Catalyzed Reactive Distillation Systems. *Ind. Eng. Chem. Res.* **1972**, *11*, 158.

(5) Hauan, S. http://www.andrew.cmu.edu/user/steinhau/Literature/access.html (accessed July 2002).

(6) Hanika, J.; Kolena, J.; Smejkal, Q. Butyl Acetate via Reactive Distillation—Modelling and Experiment. *Chem. Eng. Sci.* **1999**, *54*, 5205.

(7) Fredeslund, A.; Gmehling, J.; Rasmussen, P. *Vapor−Liquid Equilibria Using UNIFAC, a Group Contribution Method*; Elsevier: Amsterdam, 1977.

(8) Gmehling, J.; Li, J.; Schiller, M. A Modified UNIFAC Model 2. Present Parameter Matrix and Results for Different Thermodynamic Properties. *Ind. Eng. Chem. Res.* **1993**, *32*, 178.

(9) Savkovic-Stevanovic, M.; Mišic-Vukovic, M.; Boncic-Caricic, G.; Trišovic, B.; Jezdic, S. Reactive Distillation with Ion Exchangers. *Sep. Sci. Technol.* **1992**, *27*, 613.

(10) Beranek, L.; Setinek, K.; Kraus, M. Kinetics and Adsorption on Acid Catalyst. I. Gas-Phase Reesterification of Ester with Alcohols on Sulphonated Ion Exchangers. *J. Catal.* **1970**, *17*, 2265.

(11) Pöpken, T.; Geisler, R.; Götze L.; Brehm, A.; Moritz, P.; Gmehling, J. Reaction Kinetics and Reactive Distillation—On the Transfer of Kinetic Data from a Batch Reactor to a Trickled Bed. *Chem. Eng. Technol.* **1999**, *21* (5), 401.

(12) Jiménez, L.; Costa-López, J. The Production of Butyl Acetate and Methanol via Reactive and Extractive Distillation. II. Process Modeling, Dynamic Simulation, and Control Strategy. *Ind. Eng. Chem. Res.* **2002**, *41*, 6735.

(13) Castor, J.; Fair, J. R. Preparation of Tertiary Amyl Alcohol in a Reactive Distillation Column. 1. Reaction Kinetics, Chemical Equilibrium, and Mass-Transfer Issues. *Ind. Eng. Chem. Res.* **1997**, *36*, 3833.

(14) Podrebarac, G. G.; Ng, F. T. T.; Rempel, G. L. The Production of Diacetone with Catalytic Distillation. Part I: Catalytic Distillation Experiments. *Chem. Eng. Sci.* **1998**, *53*, 1067.

(15) Iborra, M.; Fité, C.; Tejero, J.; Cunill, F.; Izquierdo, J. F. Drying of Acidic Macroporous Styrene−Divinylbenzene Resins. *React. Polym.* **1992**, *21*, 65.

(16) Renon, H.; Prausnitz, J. M. Local Compositions in Thermodynamic Excess Functions for Liquid Mixtures. *AIChE J.* **1968**, *14*, 135.

(17) Hayden, J. C.; O'Connell, J. P. A Generalized Method for Predicting Second Virial Coefficients. *Ind. Eng. Chem. Process Des. Dev.* **1975**, *14*, 209.

(18) AspenTech. *Aspen PLUS Reference Manual for Release 10*; Aspen Technology Inc.: Cambridge, MA, 1998.

(19) Jiménez, L.; Espana, F. J.; Costa-López, J.; Batiu, I. Vapor−Liquid Equilibrium Data for Binary Systems Methyl Ethanoate + Butan-1-ol, Butan-1-ol + 1,2-Dimethylbenzene and Butyl Ethanoate + 1,2-Dimethylbenzene at 101.3 kPa. *ELDATA: Int. Electron. J. Phys.-Chem. Data* **1997**, *3*, 225.

(20) Jiménez, L.; Batiu, I.; Espana, F. J.; Costa-López, J. Vapor−Liquid Equilibria in Methyl Ethanoate + Butan-1-ol + 1,2-Dimethylbenzene, Butan-1-ol + Butyl Ethanoate + 1,2-Dimethylbenzene and Methanol + Methyl Ethanoate + Butan-1-ol + Butyl Ethanoate + 1,2-Dimethylbenzene at 101.3 kPa. *ELDATA: Int. Electron. J. Phys.-Chem. Data* **1998**, *4*, 49.

(21) Doherty, M. F.; Perkins, J. D. On the Dynamics of Distillation Processes. III. The Topological Structure of Ternary Curve Maps. *Chem. Eng. Sci.* **1979**, *34*, 1401.

(22) AspenTech. *Aspen SPLIT Reference Manual for Release 1*; Aspen Technology Inc.: Cambridge, MA, 1998.

(23) Momoh, S. O. Assessing the Accuracy of Selectivity as a Basis for Solvent Screening in Extractive Distillation Processes. *Sep. Sci. Technol.* **1991**, *26*, 729.

(24) Gmehling, J.; Mollmann, C. Synthesis of Distillation Processes Using Thermodynamic Models and the Dortmund Data Bank. *Ind. Eng. Chem. Res.* **1998**, *37*, 3112.

(25) Barwick, V. J. Strategies for Solvent Selection—A Literature Review. *Trends Anal. Chem.* **1997**, *16*, 293.

(26) Jiménez, L.; Costa-López, J. Solvent Selection for a Reactive and Extractive Distillation Process by Headspace Gas Chromatography. *Sep. Sci. Technol.*, manuscript accepted.

(27) Ihm, S. K.; Chung, M. J.; Park, K. Y. Activity Difference Between the Internal and External Sulfonic Groups of Macroreticular Resin Catalyst in Isobutylene Hydration. *Ind. Eng. Chem. Res.* **1988**, *27*, 41.

(28) Fromment, G.; Bischoff, K. *Chemical Reactor Analysis and Design*; Wiley Series in Chemical Engineering; John Wiley & Sons: New York, 1990.

(29) SPSS Inc. *Statistical Package for Social Science for Windows: Reference Manual (version 10)*; SPSS Inc.: Chicago, IL, 1999.

(30) España, F. J. Contribución al Estudio de la Transesterificación de Acetato de Metilo con Etanol Mediante Rectificación Reactiva Extractiva Catalítica. Ph.D. Dissertation, University of Barcelona, Barcelona, Spain, 1996.

Received for review September 12, 2001
Revised manuscript received August 21, 2002
Accepted September 19, 2002

IE0107643